Experiments show that prior to the onset of fluidization the bed behaves actually as a fluid, i.e. it presents a flat upper surface, it presents a very small resistance to an object moving in the fluidized bed, disturbances (waves), generated on the surface decay. Fluidization, vigorous movement of particles will occur when the airflow drag forces can overcome the stabilizing force of the exterior magnetic field which tends to maintain particles stationary. This has been shown in Fig. 3.

A different presentation of the results is shown in Fig. 4. Figure 4 shows the heat transfer as a function of magnetic flux density at various velocities. There are, in effect, three regimes in which magnetic field relative strength, i.e. as compared to velocity, can be classified. The first regime is a low field linear regime. The second is the onset of freezing at medium field strengths. The third is the fixed bed regime at high field strengths.

The low field regime exhibits a slight and quite linear reduction in heat transfer coefficient. In this regime, there are no observable characteristics. The inter-particle forces are small, probably alter non-observable flow patterns and reduce bubble size. The decrease in heat transfer is probably caused by those inter-particle forces.

The onset of 'freezing' is characterized by a large drop in heat transfer. Particle motion and bubbling can be seen to be greatly reduced. This is especially evident for the high flow velocities. The great reduction in particle motion increases particle residence time at the probe surface and thus reduces heat transfer.

The third regime is the fixed bed regime. This is the regime in which all particle motion stops. The heat transfer coefficient is constant as magnetic flux density is increased, and is determined by the voidage patterns established throughout the fluidized bed in the previous regime and the airflow velocity. In essence, the third regime is like the point of minimum fluidization in an unmagnetized bed. The bed exhibits fluidic characteristics and is expanded from the fixed bed state. It is more stable than the point of minimum fluidization in an unmagnetized bed, however. This is demonstrated when a perturbation to the system, such as shaking the bed, is damped out immediately; whereas, in an unmagnetized expanded bed a perturbation can cause slight bubbling. A perturbation in this regime will re-establish voidage patterns and can change the heat transfer coefficient up to a value as much as 7%.

Experiments in which the polarity of the magnetic field, i.e. the direction of the DC current flow was reversed do not indicate any effect of the polarity on heat transfer.

CONCLUSIONS

Heat transfer coefficients for a flat vertical probe in a bed of ferromagnetic particles were measured in the presence of a magnetic field. Results indicate that heat transfer is reduced as magnetic field strength is increased. The minimum fluidization velocity and the entire heat transfer vs airflow velocity curve shifts to higher velocities as the field strength is increased. The shift is caused by the need to increase the airflow drag forces to overcome the exterior field magnetic forces at the onset of fluidization.

The potential for control of fluidized bed dynamics and heat transfer processes by introducing a magnetic field is very evident in this study.

REFERENCES

1. M. Leva, *Fluidization*. McGraw-Hill, New York (1959).
2. S. S. Zabrodsky, *Hydrodynamics and Heat Transfer in Fluidized Beds*. MIT Press, Cambridge, Massachusetts (1966).
3. D. Kunii and O. Levenspiel, *Fluidization Engineering*. Wiley, New York (1969).
4. P. N. Rowe, *Fluidization* (edited by J. F. Davison and D. Harrison), pp. 121–191. Academic Press, London (1971).
5. J. S. M. Botterill, *Fluidized Bed Heat Transfer*. Academic Press, New York (1975).
6. R. Elsdon and C. J. Shearer, Heat transfer in a gas fluidized bed assisted by an alternating electric field, *Chem. Engng Sci.* **32**, 1147–1153 (1977).
7. P. W. Dietz, Heat transfer in bubbling electrofluidized beds, *Proc. Symp. on Electrohydrodynamics*, Fort Collins, Colorado (1978).
8. H. Katz and J. T. Sears, Electric field phenomena in fluidized and fixed beds, *Can. J. Chem. Engng* **47**, 50–53 (1969).
9. J. A. Agbim, A. W. Nienow and P. N. Rowe, Interparticle forces that suppress bubbling in gas fluidized beds, *Chem. Engng Sci.* **26**, 1293–1295 (1971).

Int. J. Heat Mass Transfer. Vol. 26, No. 12, pp. 1889–1892, 1983
Printed in Great Britain

0017-9310/83 $3.00 + 0.00

MIXED CONVECTION HEAT TRANSFER FROM A VERTICAL HEATED CYLINDER IN A CROSSFLOW

M. F. YOUNG and T. R. ULRICH
Department of Mechanical Engineering, University of California, Irvine, CA 92717, U.S.A.

(*Received* 27 *January* 1983 *and in revised form* 4 *April* 1983)

NOMENCLATURE

A	surface area
c_p	specific heat
d	diameter or differential
g	acceleration of gravity
Gr_L	Grashof number based on $L = \beta g(T_W - T_\infty)L^3/\nu^2$
k	thermal conductivity
L	height
m	mass
Nu_d	Nusselt number based on d
$\overline{Nu}_d$	average Nusselt number based on d
Pr	Prandtl number
$\dot{Q}$	heat transfer rate
Re_d	Reynolds number based on $d = U_\infty d/\nu$
Ri	Richardson number, Gr_L/Re_d^2
t	time
T	temperature.

Greek symbols

β	coefficient of thermal expansion
Δ	finite difference
ε	emissivity
σ	Stefan–Boltzmann constant
ν	kinematic viscosity.

Subscripts

d	based on diameter
L	based on height
w	wall condition
∞	free stream condition.

INTRODUCTION

MIXED convection external flows occur in many technological and industrial applications. Such flows result when inertial and buoyant forces have strong effects on the resulting convective transport. Applications include: electronic devices cooled by a fan, heat exchangers placed in low velocity environments, hot wire anemometers operated in low free stream velocities, and external solar central receivers exposed to wind currents.

Mixed convection studies can be loosely classified by the relative angle that the free stream velocity vector makes with the gravitational force, e.g. aided, opposed, or orthogonal mixed convection. To date, only a few analytical studies of orthogonal mixed convection from vertical surfaces have been completed. This is probably due to its three-dimensional nature. One of the first analytical three-dimensional laminar mixed convection studies from a vertical flat plate was conducted by Young and Yang [1]. A perturbation technique was used in ref. [1] to investigate the effect of a small crossflow on a dominant buoyant flow. Evans, and Plumb [2] also studied orthogonal laminar mixed convection from an isothermal vertical flat plate by using a stream function transformation of the describing partial differential equations. Orthogonal laminar mixed convection from a vertical cylinder was studied by Yao and Chen [3] using an asymptotic solution. Their results are limited to small values of the local aspect ratio divided by the square root of the Richardson number.

Few investigators have measured mixed convection heat transfer coefficients from vertical surfaces in a crossflow. Among them, Oosthuizen and Leung [4] investigated orthogonal mixed convection from a vertical cylinder with height to diameter ratios between 8 and 16. The Grashof number range investigated in ref. [4] was about 10^7–10^8, while the Reynolds number was varied from 100 to about 1600. In another study, Oosthuizen and Madan [5] investigated the effect of angle between the free stream velocity and the buoyant force vectors on the mixed convection heat transfer from a cylinder. It was found in ref. [5] that for assisting (0°) and orthogonal (90°) flows, the buoyant force increased the heat transfer rate above that which would result at the same Reynolds number in pure forced convection. For larger angles, i.e. 135° and 180°, the opposite was found.

The mixed convection heat transfer coefficient from smooth vertical cylinders placed in a crossflow is measured in the present study. The cylinders are operated at overheat ratios between 2 and 3. The Grashof number, Gr_L, range investigated is 10^7–10^9 while the Reynolds number, Re_d, is varied from 10^4 to 10^5.

EXPERIMENTAL PROCEDURE

Apparatus

Three models with height, L, to diameter, d, ratios of 2, 4.5, and 9 are tested in the present study. Cylinder heights and diameters are listed in Table 1. The models are hollow aluminum cylinders and are fitted with insulating ends. Heater elements (nichrome wire) are inserted down axial holes which are drilled at several locations around the cylinder. Thermocouples are placed at several axial locations around each cylinder surface. Thermocouples are also suspended at various heights along each cylinder centerline to measure end losses. The interior of the cylinders are filled with liquid foam insulation and allowed to harden. A diagram of a model is shown in Fig. 1. Details are given in ref. [6].

Table 1. Model dimensions

Model	Height, cm (in.)	Diameter, cm (in.)	L/d	Blockage correction applied to the Reynolds number
1	10.16 (4)	5.08 (2)	2	1.05
2	22.86 (9)	5.08 (2)	4.5	1.11
3	22.86 (9)	2.54 (1)	9	1.05

The models are mounted vertically in an elevated, blow down, cryogenic wind tunnel† with a 304.8 × 304.8 mm (1 × 1 ft) test section. The working fluid is gaseous nitrogen. The wind tunnel is operated at about 0.106 MPa (15.4 psia) and about 139 K (250°R). The velocity and temperature profiles are uniform to within ±1% and the turbulence intensity is less than 0.03%. The use of a cryogenic wind tunnel eliminates many of the difficulties associated with operating small aspect ratio models at large overheat ratios in high Grashof and Reynolds numbers flows. The advantages of performing mixed convection studies in a cryogenic environment are discussed by Clausing [7]. The advantages are: (1) a significant increase in the Grashof number can be obtained through a decrease in the viscosity and through increases in the density, the coefficient of expansion, and the driving temperature difference, (2) a significant increase in the Reynolds number can be accomplished through an increase in the density and a decrease in the viscosity, and (3) radiative effects can be made small even for large overheat ratios since free stream temperatures and hence model temperatures are low.

Modeling requirements

Proper modeling between a prototype and its model requires geometric, dynamic, and thermal similarity. The important dimensionless groups are determined by a dimensional analysis of the mass, momentum, energy, and property relationships. By assuming that the model is held at a constant temperature, T_w, in a uniform velocity and temperature environment, U_∞ and T_∞, that the model is smooth, and that the model is fixed relative to the free stream velocity and gravitational force vectors, a dimensional analysis shows that the local Nusselt number is a function of:

$$Nu_d = Nu_d(D^*, Re_d, Gr_L/Re_d^2, Pr, T_w/T_\infty, L/d), \quad (1)$$

where D^* is a dimensionless coordinate denoting the location where the Nusselt number is being measured. The functional form in equation (1) is not unique since the Richardson number, Gr_L/Re_d^2, can be replaced by the Rayleigh number or the Froude number. The analytical studies of refs. [1–4] indicate, however, that the Richardson number is a useful choice. If the present results are limited to air and if only the average Nusselt number is of interest, equation (1) reduces to:

$$\overline{Nu}_d = \overline{Nu}_d(Re_d, Gr_L/Re_d^2, T_w/T_\infty, L/d). \quad (2)$$

The dimensionless groups in equation (2) are of interest in the present study and can be varied over the desired range using a cryogenic wind tunnel.

Data reduction

The mixed convection heat transfer rate can be measured by performing an energy balance on the cylinder. The wind tunnel is operated at a particular velocity setting, and the cylinder is heated. When the cylinder reaches about 80–120°C, the heater is turned off and the heat transfer tests started. For the case

† The wind tunnel is located at the McDonnell-Douglas Aerophysics Laboratory, El Segundo, California.

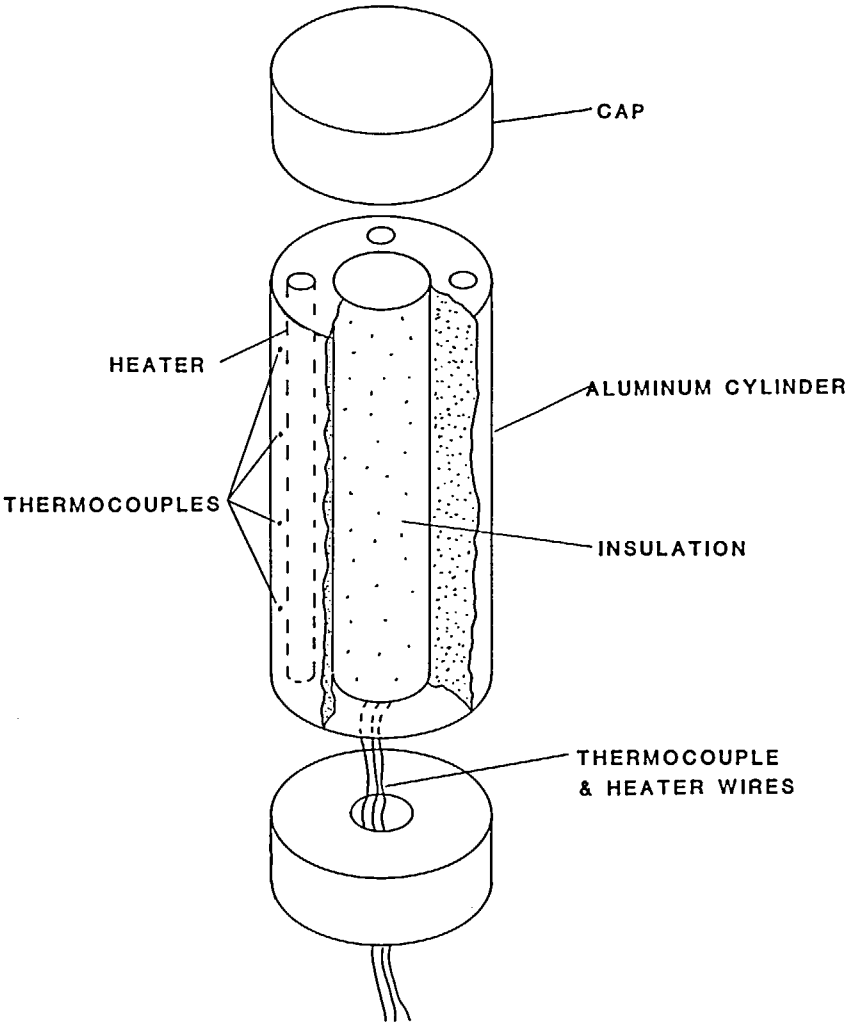

FIG. 1. Model configuration.

when the heater power is zero, an energy balance gives:

$$\dot{Q}_{\text{convection}}^{\text{mixed}} = -mc_p\frac{dT}{dt} - \varepsilon\sigma A(T_w^4 - T_\infty^4) - \dot{Q}_{\text{end losses}}. \quad (3)$$

The cylinder emissivity is estimated from tabulated data to be 0.11. Exact specification is unnecessary since the radiation term is small. The cylinder and insulation temperatures are recorded by a data acquisition system (HP-9826 and HP-3497A). Consequently, by monitoring the rate of decay of the cylinder temperature, the free stream temperature, and the insulation temperatures, equation (3) can be solved for the mixed convection heat transfer rate. The Nusselt number is then calculated at any instant of time from:

$$\overline{Nu}_d = \dot{Q}_{\text{convection}}^{\text{mixed}}\{d/[Ak(T_w - T_\infty)]\}. \quad (4)$$

The cylinder temperatures are uniform at any particular time, to within $\pm 0.5°C$. The loss term, $\dot{Q}_{\text{end losses}}$, is less than 3% of the total heat loss. The mass of the cylinder is measured with a precision mass balance to within ± 0.1 g. An error analysis indicates that the measured heat transfer coefficients are accurate to within $\pm 5\%$.

RESULTS

Model 1 ($L/d = 2$) is attached at its bottom end to the test section via an aerodynamic shaped sting while Models 2 ($L/d = 4.5$) and 3 ($L/d = 9$) are secured to the test section at each of its ends with 3.8 cm (1.5 in.) insulating caps. Consequently, Model 1 is hydrodynamically and thermally finite while Models 2 and 3 are hydrodynamically infinite and thermally finite (see ref. [6]).

Using the procedure outlined in the previous section, the free and forced convection limits were checked. The present results are in agreement with the forced convection correlation presented in Douglas and Churchill [8] and the free convection correlation presented in Nagendra *et al.* [9]. With the models in place, the cryogenic wind tunnel is operated at different free stream velocities and temperatures. The average Nusselt number correlation for the three models is shown in Fig. 2. The thermal boundary condition simulated, at a particular time, is that of a constant wall temperature. The results in Fig. 2 are corrected for model blockage effects using the ratio of the test section area to the mean flow area as noted in Perkins and Leppert [10]. The blockage corrections applied to the Reynolds numbers are listed in Table 1. The fluid properties used in the Nusselt, Reynolds, and Grashof numbers are evaluated at the film temperature, $T_f = (T_w + T_\infty)/2$.

The non-dimensional parameters† used to correlate the

†The authors wish to acknowledge that a reviewer suggested these parameters.

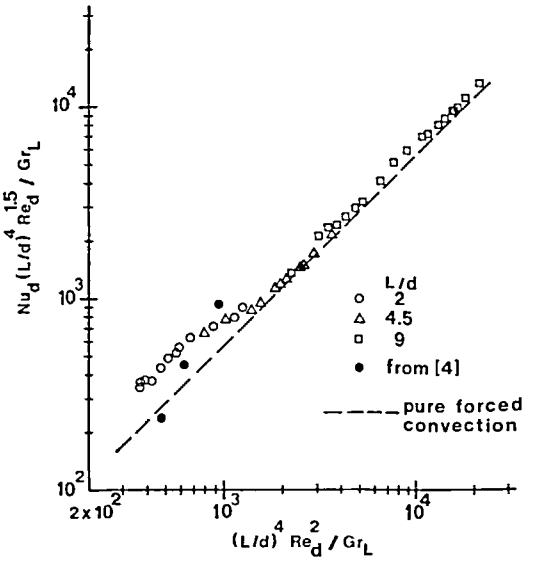

FIG. 2. Mixed convection heat transfer results for different aspect ratios.

data in Fig. 2 are suggested from equation (23) in Yao and Chen [3]. They can be found by integrating the first term of the local Nusselt number in ref. [3] over the cylinder and then changing the length scale in the Grashof number to the cylinder height. The dotted line shown in Fig. 2 is the pure forced convection limit. It is found by rewriting the ordinate as:

$$\frac{Nu_d}{\sqrt{Re_d}}\{(L/d)^4 Re_d^2/Gr_L\},$$

and using the forced convection correlation for $Nu_d/\sqrt{Re_d}$ in ref. [8].

The present results approach the pure forced convection limit for $(L/d)^4 Re_d^2/Gr_L$ greater than about 1500. Below this value of $(L/d)^4 Re_d^2/Gr_L$, free convection adds between 20–50% to the pure force convection results. The data in Fig. 2 can be represented by the following expressions to within ±5%:

$$\frac{Nu_d}{\sqrt{Re_d}} = 0.56 \quad \text{for } (L/d)^4 Re_d^2/Gr_L \geqslant 1500, \tag{5a}$$

$$\frac{Nu_d}{\sqrt{Re_d}} = 25\{(L/d)^4 Re_d^2/Gr_L\}^{-1/2}$$

$$\text{for } 700 < (L/d)^4 Re_d^2/Gr_L < 1500, \tag{5b}$$

$$\frac{Nu_d}{\sqrt{Re_d}} = 0.943 \quad \text{for } 350 \leqslant (L/d)^4 Re_d^2/Gr_L \leqslant 700, \tag{5c}$$

valid for:

$$0.02 < Gr_L/Re_d^2 < 3.0,$$

$$5\times10^3 < Re_d < 7\times10^4,$$

$$10^7 < Gr_L < 10^9,$$

$$2 < T_w/T_\infty < 3.$$

Also shown in Fig. 2 are results calculated from the data of Oosthuizen and Leung [4]. The data from ref. [4] follow the trends of the present results. Discrepancies between the results of ref. [4] and the present data can be attributed to: (1) extrapolation errors in reading data from the plots of ref. [4] and (2) the difference in overheat ratios between the two studies. An overheat ratio of about 1.2 was investigated in ref. [4] while in the present study, the overheat ratio is between 2 and 3. Further studies are needed to determine the dependence of Nusselt number on overheat ratio.

Acknowledgements—This study was supported by the Thermodynamics, Environment, and Biotechnology Department, McDonnell-Douglas Astronautics Company, Huntington Beach, California, and the Committee on Research, University of California, Irvine.

REFERENCES

1. R. J. Young and K. T. Yang, Effect of small cross flow and surface temperature variation on laminar free convection along a vertical plate, *J. Appl. Mech.* **30**, 252–256 (1963).
2. G. H. Evans and O. A. Plumb, Laminar mixed convection from a vertical heated surface in a crossflow, *J. Heat Transfer* **104**, 554–558 (1982).
3. L. S. Yao and F. F. Chen, A horizontal flow past a partially heated infinite vertical cylinder, *J. Heat Transfer* **103**, 546–551 (1981).
4. P. H. Oosthuizen and R. K. Leung, Combined convective heat transfer from vertical cylinders in a horizontal flow, ASME Winter Annual, 78-WA/HT-45 (1978).
5. P. H. Oosthuizen and S. Madan, The effect of flow direction on combined convective heat transfer from cylinders to air, *J. Heat Transfer* **93**, 240–242 (1971).
6. M. F. Young, Convective losses from right circular solar central receivers, Final Report for McDonnell-Douglas Astronautics Company, Project 82614247 H (1982).
7. A. M. Clausing, Advantages of a cryogenic environment for experimental investigations of convective heat transfer, *Int. J. Heat Mass Transfer* **25**, 1255–1257 (1982).
8. W. J. M. Douglas and S. W. Churchill, Recorrelation of data for convective heat transfer between gases and single cylinders with large temperature differences, *Chem. Engng Symp. Ser.* **52**, 23–28 (1956).
9. H. R. Nagendra, M. A. Tirunarayanan and A. Ramachandran, Laminar free convection from vertical cylinders with uniform heat flux, *J. Heat Transfer* **92**, 191–194 (1970).
10. H. C. Perkins and G. Leppert, Forced convection heat transfer from a uniformly heated cylinder, *J. Heat Transfer* **84**, 157–263 (1962).